

# Hierarchically Porous Carbon Foams from Pickering High Internal Phase Emulsions

*Robert T. Woodward,<sup>a,\*</sup> Derrick W. H. Fam,<sup>b</sup> David B. Anthony,<sup>b</sup> Jindui Hong,<sup>a</sup> Tom O. McDonald,<sup>c</sup> Camille Petit,<sup>a</sup> Milo S. P. Shaffer<sup>b</sup> and Alexander Bismarck<sup>a,d</sup>*

<sup>a</sup> Department of Chemical Engineering, Imperial College London, South Kensington Campus, London, SW7 2AZ, United Kingdom

<sup>b</sup> Department of Chemistry, Imperial College London, South Kensington Campus, London, SW7 2AZ, United Kingdom

<sup>c</sup> Department of Chemistry, University of Liverpool, Crown Street, Liverpool, L69 7ZD, United Kingdom

<sup>d</sup> Polymer and Composite Engineering (PaCE) Group, Institute of Materials Chemistry & Research, Faculty of Chemistry, University of Vienna, Währingerstraße 42. 1090 Vienna, Austria

## Abstract

Carbon foams were produced from a macroporous poly(divinylbenzene) (poly(DVB)) precursor, synthesized by polymerizing the continuous but minority phase of water-in-oil high internal phase emulsions (HIPEs) stabilized by molecular and/or particulate emulsifiers. Both permeable and non-permeable hierarchically porous carbon foams, or ‘carboHIPEs’, were prepared by carbonization of the resulting macroporous polymers at 800 °C. The carbon yields were as high as 26 wt.% of the original polymer. CarboHIPEs retain the pore structure of the macroporous polymer precursor, but with surface areas of up to 505 m<sup>2</sup>/g and excellent electrical conductivities of 81 S/m. Contrary to some previous reports, the method does not require further modification, such as sulfonation or additional crosslinking of the polyHIPE prior to carbonization, due to the inherently crosslinked structure of poly(DVB). The use of a pourable, aqueous emulsion-template enables simple moulding, minimises waste and avoids the strong acid treatments used to remove many conventional solid-templates. The retention of the macroporous structure is coupled with the introduction of micropores

\*Corresponding author

e-mail address: [r.woodward@imperial.ac.uk](mailto:r.woodward@imperial.ac.uk) (R. Woodward)

during carbonization, producing hierarchically porous carboHIPEs, suitable for a wide range of applications as sorbents and electrodes.

## 1. Introduction

Porous carbonaceous materials have importance for a huge range of applications including catalyst support [1, 2], gas separation [3, 4], electromagnetic interference shielding [5, 6], water purification [7], and energy storage devices such as supercapacitor devices [8, 9] and Li-ion batteries [10, 11]. Such materials have an abundant range of precursors and display many advantages such as relatively low cost, low density and solvent and electrochemically resistance [12, 13]. One potential route to monolithic porous carbon structures is *via* the pyrolysis of macroporous polymers synthesised from high internal phase emulsion (HIPE) systems, so called polyHIPEs [14]. A HIPE is defined as an emulsion system with an internal phase volume fraction exceeding 0.74, the maximum packing fraction of monodisperse spheres. The formation of polyHIPEs involves the polymerisation of the continuous, yet minority, monomer phase of the emulsion, usually containing a small amount of cross-linker. This polymerization is followed by the removal of the internal phase template in order to produce a free-standing, monolithic porous polymer [14, 15]. Despite the vast breadth of work reported on both polyHIPEs and porous carbons, only a relatively small number of reports have described the preparation of structured carbonaceous porous materials from polyHIPE precursors. Existing precursors include polyHIPEs based on polyacrylonitrile (PAN) [16], tannins [17], lignin [18], silica foams [19, 20] and resorcinol-formaldehyde [21-23] amongst others [24-26]. Styrene-co-divinylbenzene (ST-co-DVB) polymers are particularly well-studied polyHIPE materials due to their relatively simple synthesis [27, 28]. However, in order for these materials to survive carbonization they require further treatment prior to heating. For example, when combined with up to 40 % vinylbenzyl chloride (VBC, used to control pore size), poly(ST-co-DVB)HIPEs have been successfully converted into porous carbons at high temperatures after stabilisation by sulphonation [29]. Similar systems employ VBC as a crosslinkable functional group, enabling hypercrosslinking

of poly(ST-co-DVB)HIPEs via Friedel-Crafts alkylation, again allowing for the production of porous carbons [30]. Not only does the inclusion of chlorine bring about the evolution of toxic gases upon carbonization but these secondary reactions increase the cost and complexity of these systems and introduce purification and process challenges when applied to bulk porous polyHIPEs. To avoid these problems, an inherently more stable polyHIPE is needed. In this paper, we combine two strategies to enable the simple production of both open- and closed-cell carbonaceous monoliths exhibiting hierarchical porosity via the pyrolysis of poly(DVB)HIPEs produced by polymerization of particulate stabilised w/DVB HIPEs.

DVB is a bifunctional monomer widely used as a cross-linking agent in the formation of poly(ST-co-DVB)HIPEs. The addition of DVB enables the production of insoluble networks by cross-linking linear polystyrene chains, leading to polymers with greatly improved stability [31-33]. DVB is also a well known precursor for carbonaceous materials, for example it has previously been utilized for the synthesis of carbon nanocapsules [34] or of carbon foams [35], in both cases templated around inorganic constructs. However, these materials require complex preparation such as the removal of the solid templates by HF treatment to etch away the templates post-pyrolysis [34]. By employing DVB as the sole monomer to produce poly(DVB)HIPEs from simple water-in-oil (w/o) HIPE templates, a macroporous carbon precursor can be created. This provides a simple process for the production of carbon foams, eliminating the need for further treatments and allowing for the simple removal of the aqueous template prior to carbonization.

It has been well reported that the structure of polyHIPEs is controlled by the phase volume ratio of the emulsion template, the choice of emulsifier and emulsification method [15, 36-38]. The use of molecular surfactants usually results in small droplet diameters. During polymerization, ruptures can occur at the thinnest points of the film between droplets, leading to a highly interconnected pore structure, and hence permeable polyHIPEs [15, 39]. Previous reports suggest that some molecular surfactants act as precipitant porogens during the polymerization of a DVB continuous phase, forming a secondary pore structure within the walls of the resulting polyHIPE [31, 32]. This dual structuring

role leads to polymers with increased porosities and higher surface areas. In contrast to molecular surfactants, particulate emulsifiers generally stabilise larger droplets. Upon polymerisation, film ruptures are less likely to occur, yielding non-permeable, or closed-cell structures with few or no pore throats [37, 38, 40]. However, these Pickering-HIPE templates can be modified to produce open-cell and therefore permeable polyHIPEs, by addition of a suitable surfactant after generating the initial Pickering-HIPE [41]. Poly(DVB)HIPEs produced by the polymerization of surfactant, particle, and mixed surfactant/particle-stabilized w/o HIPE templates were carbonized, in order to explore the simple formation of conducting, hierarchically porous carboHIPEs.

## **2. Experimental Section**

### ***2.1. Materials***

Divinylbenzene (80 %), CaCl<sub>2</sub>, azobisisobutyronitrile (AIBN), ethanol, and Span 80 were all purchased from Sigma Aldrich. Hypermer 2296 was kindly supplied by Croda. Hydrophobic silica particles (HDK grade H20) were kindly provided by Wacker Chemie. The hydrophobicity of the particles is derived from the silanization of hydrophilic fumed silica, resulting in silica containing only 50 % the silanol content measured in that of the hydrophilic precursor (around 1 x SiOH/nm<sup>2</sup> in the hydrophobic particles). Silver paint was purchased from Agar Scientific. All products were used as received.

### ***2.2. Preparation of HIPEs and subsequent poly(DVB)HIPEs***

For a typical Pickering HIPE, silica nanoparticles (90 mg, 3 wt. %) were weighed and added to DVB (3 mL) before shaking the sample by hand for 5 min in order to disperse the particles in the monomer. AIBN (1 mol % with respect to the monomer, 35 mg) was then added and the mixture gently stirred using a vortex mixture (Vortex-Genie 2, speed setting '3', equating to roughly 600 rpm) before an

aqueous CaCl<sub>2</sub> solution (10 g/L, 9 mL) was added slowly over 20 min while still stirring using the vortex mixer at the same speed setting. All HIPEs comprised of 75 vol.% aqueous phase and 25 vol.% organic phase in order to yield macroporous polymers with  $\geq 75$  % porosity. After the addition of the aqueous phase was complete, the resulting emulsion was stirred more vigorously (speed setting '10', roughly 3000 rpm) for a further 5 min before the HIPE was transferred into a 15 mL free standing polypropylene centrifuge (Falcon) tube and heated at 70 °C for 24 h in a convection oven to initiate polymerization. For the molecular surfactant stabilized HIPEs, 20 vol.% of the surfactant was added with respect to the initial monomeric phase, but otherwise the procedure was the same. After polymerization, the polyHIPE was removed from the Falcon tube and washed three times in an ethanol bath for 2 h at a time. The structure was then dried in a vacuum oven at 110 °C overnight. PolyHIPEs formed from Span 80-stabilised HIPEs are denoted as sPH1, those from Hypermer 2296-stabilised HIPEs as sPH2, with the 's' denoting the use of molecular surfactants. PolyHIPEs from solely silica nanoparticle-stabilised HIPEs are denoted as pPH3 and when formed from a HIPE stabilised by both silica nanoparticle and the molecular surfactant Hypermer 2296, as psPH4, the 'p' denoting the use of a particulate emulsifier.

### **2.3. Preparation of carboHIPEs**

The poly(DVB)HIPE's volumes were initially measured and the materials weighed before being placed in a chamber furnace (Lenton ECF 12/30) fitted with an air tight Inconel metal retort (Lenton A105). Samples were degassed in the furnace at room temperature for 30 min under a constant flow of N<sub>2</sub> (1 L/min). After degassing, the samples remained under a constant flow of N<sub>2</sub> and were carbonized by heating to 800 °C at a ramp rate of 5 °C/min. The sample was then held at 800 °C for 30 min before being allowed to cool slowly to room temperature. After this time, the volume of samples were again measured and the resulting carbon weighed in order to determine the volume shrinkage and carbon yield. The carbonized samples are denoted with the same notations as

mentioned in section 2.2., using 'c' as a suffix. The production of each material was repeated at least three times to assess the reproducibility of their synthesis.

#### **2.4. Characterization of materials**

The N<sub>2</sub> isotherms and BET surface area of each sample were measured on a Micromeritics 3Flex Surface Characterization Analyzer at -196 °C. Each sample (minimum 50 mg) was degassed *in-situ* under vacuum (around 0.0030 mbar) at 120 °C for at least 4 h prior to the measurement. SEM images, with the exception of the high magnification images in Figure 1, were taken on a variable pressure SEM (JEOL JSM 5610 LV (0.5-35 kV)). The high-resolution images were obtained using a high resolution field emission gun SEM (FEGSEM (5 kV, InLens detector)) (Leo Gemini 1525 coupled with SmartSEM software interface, Carl Zeiss NTS Ltd., UK). All polyHIPE samples were fixed on Al stubs (Agar Scientific Ltd., UK) using silver dag used to attach samples securely. Silica particles alone were imaged by firstly dispersing in acetone (0.001 wt. %) and subsequently drop-casting the solution on to a glass slide stuck to an Al stub using carbon tape. All samples were coated with gold (10 nm) once mounted on to stubs, prior to imaging. Image analysis, such as measuring average pore diameter of polyHIPEs was carried out using the image software ImageJ (version 1.48) [42]. For electrical conductivity measurements, a cylindrical monolithic sample of either a polyHIPE or the subsequent carboHIPE was placed between two flat headed probes (261-5109, RS-Components Ltd., UK) and the resistivity measured by impedance spectroscopy (IS) using a potentiostat (Gamry Instruments REF600-23011, initial frequency 10 kHz, final frequency 1 Hz, AC voltage 10 mV rms). To reduce signal noise from external sources, measurements were taken inside a Faraday cage (Spacial CRN IP66, Schneider Electric). The samples were painted using silver dag at either end of the cylinder in order to minimise contact resistance between the sample surface and the probes. The silver paint was applied as thick paste in order to prevent significant permeation into the sample. The conductivity was calculated using the resistance measured in the linear region at frequency 100 Hz ( $R$ ,  $\Omega$ ) through the sample, the monolith cross-sectional area and the monolith length. Raman

spectroscopy was carried out on a Renishaw inVia micro-Raman spectrometer using a 633 nm laser with 1800 lines/mm grating. A total of five spectra were collected for each sample and were background corrected, collated and then normalised to demonstrate average Raman spectra for each. Skeletal density  $\rho_s$  was measured on powdered polyHIPE samples (0.5 g) using He (BOC, UK) displacement pycnometry (AccuPyc 1330, Micromeritics Ltd., U.S.A.) with fill pressure of 19.5 psig. At least 10 measurements were taken and the average value recorded. Thermogravimetric analysis was performed on a thermobalance (TG 209 F1 Libra, Netzsch) with a ramp rate of 10 °C in a N<sub>2</sub> atmosphere, using a minimum of 10 mg of sample. The envelope density  $\rho_e$  was calculated simply by using the mass  $m$  and volume  $V$  of cylindrical monoliths of each material ( $\rho_e = m/V$ ). The percentage porosity  $P$  was then determined using both the envelope and skeletal density ( $P = (1 - \rho_e/\rho_s) \times 100 \%$ ).

### ***3. Results and Discussion***

Initially, three poly(DVB)HIPEs were synthesized by polymerization of water-in-oil (w/o) HIPEs stabilized by different emulsifiers to identify the most robust polyHIPE precursor for producing carbon foams. The HIPEs were stabilized using either standard molecular surfactants (Span 80 or Hypermer 2296), or hydrophobised fumed silica nanoparticles. All emulsions consisted of a water immiscible DVB continuous phase containing 1 mol% of the free-radical initiator, AIBN, and an aqueous phase containing CaCl<sub>2</sub> (10 g/L), their formulation is described in more detail in the Experimental Section, 2.2. Photographs of these initial emulsions are shown in Figure S1a. The particle stabilized HIPE appeared more viscous when compared to the surfactant stabilized HIPEs (as demonstrated by tube inversion of the as formed HIPEs in Figure S2). Optical microscope images of the as prepared emulsions show droplet sizes that are in rough agreement with the emulsion-templated macropores in the resulting polyHIPEs, suggesting little or no coalescence occurred during

polymerization (Figure S3). All emulsions appeared stable; the surfactant stabilized HIPEs showed only a small amount of separation after up to 24 h (Figure S1b,c).

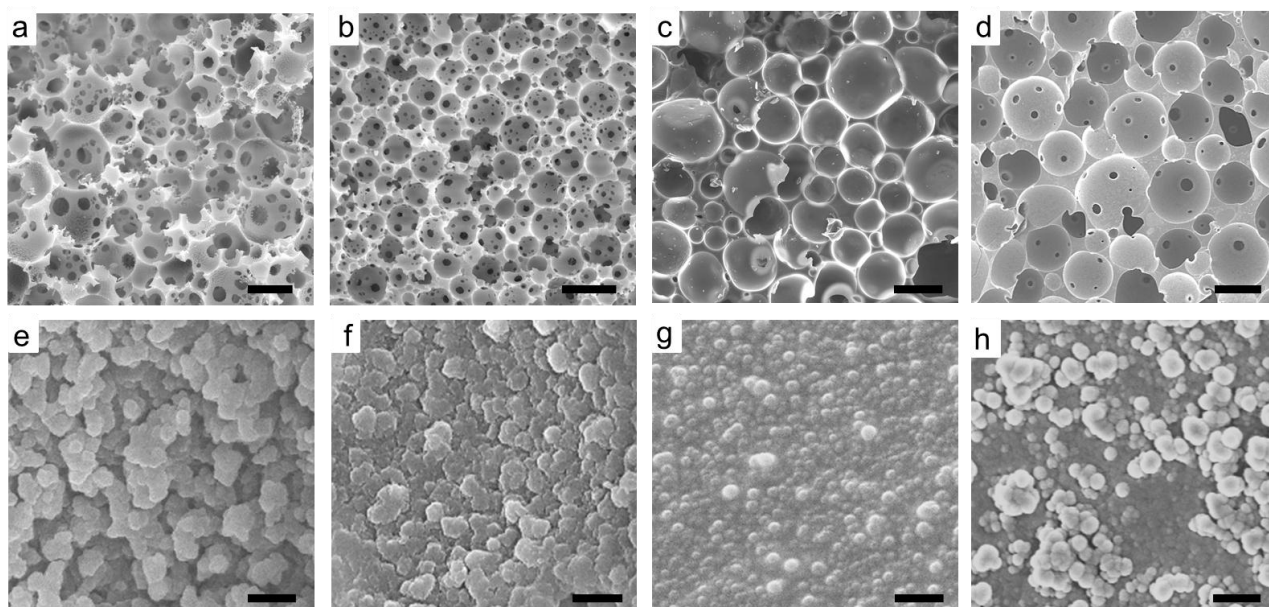


**Figure 1** SEM images of poly(DVB)HIPEs prepared by polymerization of a HIPE stabilized by a) Span 80 (sPH1), b) Hypermer 2296 (sPH2), c) hydrophobised silica particles (pPH3), and d) both Hypermer 2296 and hydrophobised silica particles (psPH4). (e) – (h) are high magnification SEM images of sPH1, sPH2, pPH3 and psPH4, respectively. Scale bars represent 20  $\mu\text{m}$  in (a) and (b), 80  $\mu\text{m}$  in (c) and (d) and 500 nm in (e) – (h).

Heating the HIPEs for 24 h at 70 °C in a convection oven yielded poly(DVB)HIPEs in all cases (properties summarised in Table 1). SEM images of the poly(DVB)HIPEs produced from Span 80 stabilized HIPEs (sPH1) and Hypermer 2296 stabilized HIPEs (sPH2) show open-cell interconnected structures with pores remaining in the place of removed droplets of internal phase (Figure 1a and b). sPH1 possessed an average macropore diameter of  $17 \pm 7 \mu\text{m}$ , while the macropores of sPH2 were only slightly smaller with average diameters of  $10 \pm 4 \mu\text{m}$ . On the other hand, the polyHIPEs produced from particle stabilised HIPEs (pPH3) were closed-cell and possessed larger average macropore diameters of  $69 \pm 28 \mu\text{m}$  (Figure 1c); increased pore diameter and decreased permeability are expected when using particulate emulsifiers [40, 41]. The thin films of continuous phase in the particle stabilized HIPEs form few or no interconnecting pore throats after polymerisation to pPH3 (Figure 1c), likely due to the more stable w/o interface formed in the initial HIPE *via* the effectively irreversible adsorption of particles [43]. High magnification SEM images of the poly(DVB)HIPEs



show some secondary porosity in the walls of both sPH1 and sPH2 (Figure 1e,f). The observed porosity in the walls of the polyHIPE is generated by the molecular surfactant also acting as a porogen, an effect that has previously been shown to provide the materials with pores in both the meso- (2 nm – 50 nm) and macropore (>50 nm) range [31, 32]. This inherent porosity was not observed in the walls of pPH3 (Figure 1g), as the particulate emulsifiers do not act as precipitant porogens. The spherical objects at the surface of the pore walls (Figure 1g) were of similar diameter with that of the particulate emulsifiers (Figure S4). These diameters were  $70 \pm 18$  nm and  $75 \pm 25$  nm, respectively, suggesting that these objects are in fact the particulate emulsifiers. In order to form an interconnected poly(DVB)HIPE (psPH4, Figure 1d) from a particle stabilized HIPE, a small amount of Hypermer 2296 was added to the already-formed emulsion (images of the emulsion immediately after production and after 24 hours are shown in Figure S5). It has been previously demonstrated that upon gentle stirring, the surfactant (Hypermer 2296) partially replaces the hydrophobic silica particles at the interface [44], resulting in the formation of pore throats during polymerization of the continuous phase. The secondary pore structure observed in the walls of sPH1 and sPH2 is not as apparent as in psPH4, which still appears to have a good coverage of silica nanoparticles (Figure 1h, S6). The SEM images of psPH4 appear to show some larger spheres at the surface of the polymer. These spheres may be a result of aggregation of silica particles due to some removal of particles from the w/o interface by the molecular surfactant prior to polymerization, however they could also be polymer spheres as a result of the small amount of added molecular surfactant acting in part as a porogen.

**Table 1.** Properties of initial polyHIPEs and carboHIPEs (pPH3 & psPH4) after pyrolysis.

Structure (emulsifier)	Macropore diameter ( $\mu\text{m}$ ) <sup>a</sup>	BET surface area ( $\text{m}^2/\text{g}$ ) <sup>b</sup>	Porosity (%) <sup>c</sup>	Skeletal density ( $\text{g}/\text{cm}^3$ )	Envelope density ( $\text{g}/\text{cm}^3$ )	Conductivity (S/m)
sPH1 (Span 80)	$17 \pm 7$	40	$84.0 \pm 0.4$	1.11	$0.18^e$	N/A <sup>f</sup>
sPH2 (Hypermer 2296)	$10 \pm 4$	21	$82.4 \pm 0.3$	1.12	$0.20^e$	N/A <sup>f</sup>
pPH3 (silica particles)	$69 \pm 28$	<1	$79.1 \pm 1.1$	1.11	$0.23 \pm 0.01$	N/A <sup>f</sup>
psPH4 (silica particles)	$77 \pm 35$	50	$78.4 \pm 1.1$	1.09	$0.24 \pm 0.01$	N/A <sup>f</sup>
pPH3c CarboHIPE	$54 \pm 26$	505	$89.5 \pm 1.4$	1.55	$0.16 \pm 0.02$	$35.2 \pm 1.5$
psPH4c CarboHIPE	$50 \pm 20$	115 <sup>d</sup>	$89.4 \pm 1.3$	1.83	$0.19 \pm 0.02$	$80.7 \pm 1.2$

<sup>a</sup> Measured using the image analysis software imageJ. <sup>b</sup> Calculated from  $\text{N}_2$  sorption isotherms measured at 77 K. <sup>c</sup> Porosity calculated using the mass and volume of cylindrical monoliths (see equation (1)). <sup>d</sup> Calculated from an argon sorption isotherm measured at 77 K. <sup>e</sup> Errors not quoted as they are  $< \pm 0.01 \text{ g}/\text{cm}^3$ . <sup>f</sup> Conductivities all measured below the lower limit of the recording equipment, rendering them non-conductive.

BET analysis showed sPH1, sPH2 and psPH4 to have interconnected pore structures, with surface areas typical of poly(DVB)HIPEs, whilst pPH3 was confirmed to be closed-cell with no measurable surface area (Table 1). Both sPH1 and sPH2 exhibited type IV isotherms with some hysteresis upon desorption (Figure 2a). The hysteresis is suggestive of capillary condensation, indicating the presence of some mesoporosity. This mesoporosity and larger surface areas measured in sPH1 and sPH2 derive from the inherent, secondary pore structure within the poly(DVB)HIPE walls (Figure 1e,f) [45]. The lack of a secondary pore structure in pPH3 is also evident in its BET isotherm, with the sample displaying a lack of any significant  $\text{N}_2$  adsorption (Figure 2b). The psPH4 isotherm also showed some mesoporosity in spite of the large emulsion-templated macropore diameter (Figure 2b), in good agreement with the SEM images (Figure 1h and S3) in which some larger spherical objects, possibly silica particle aggregates or polymer spheres, were observed in the walls of the polymer. The absence of any steep  $\text{N}_2$  uptake at low relative pressures indicated a lack of any significant microporosity in any of the poly(DVB)HIPEs. As expected, all polyHIPEs had very similar skeletal densities of 1.11-1.12  $\text{g}/\text{cm}^3$  (Table 1).

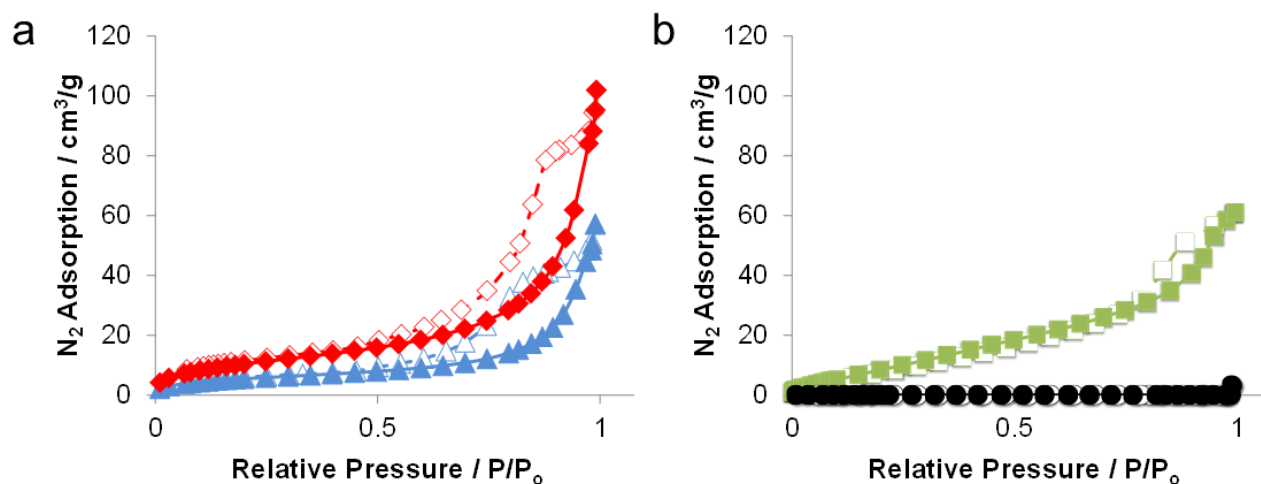


**Figure 2** BET N<sub>2</sub> isotherms of polyHIPEs a) derived from molecular surfactant HIPEs, sPH1 (red diamonds) and sPH2 (blue triangles) and b) derived from particle stabilized HIPEs, pPH3 (black circles) and psPH4 (green squares). Filled shapes show adsorption curves, while empty shapes show desorption curves.

To produce carboHIPEs, all samples were heated at a ramp rate of 5 °C/min to 800 °C in an inert N<sub>2</sub> atmosphere. They were held at this temperature for 30 min before being allowed to cool slowly to room temperature. Photographs of all four poly(DVB)HIPEs before and after carbonization (Figure 3a-d) show that carboHIPEs produced from pPH3 (pPH3c) and psPH4 (psPH4c) (Figure 3c,d, respectively) retained their monolithic structure much more successfully than carbonized sPH1 (sPH1c) and sPH2 (sPH2c), which collapsed during heating (Figure 3a,b, respectively). Upon carbonization, materials became much more brittle than the polyHIPE precursors, however they were still handled easily without damaging the samples. It is worth noting that the inclusion of styrene in the polyHIPE precursors was also investigated, however upon carbonization it was found to be detrimental to the templated porosity in materials containing up to 80 wt.% DVB. Therefore it was decided that using DVB as the sole-monomeric component is not only more efficient when producing carboHIPEs, but also simplifies their synthesis. After carbonization 26 ± 1 % and 21 ± 2 % of pPH3c and psPH4c's initial weight remained, respectively, while both sPH1c and sPH2c retained only 8-9 % of their initial weight. This difference is, in part, due to the remaining inorganic silica nanoparticle content in carboHIPEs derived from particle-stabilized HIPEs, determined to be 14.6 wt.% in pPH3c by thermogravimetric analysis (Figure S7). However, even accounting for this there is a greater pure

carbon yield in the particulate-stabilised systems. This increased carbon yield could be a product of the framework of silica particles providing some further stability to the system during heating, preventing not only collapse of the macropores but also producing a better carbon yield. However, this result was nevertheless surprising and deserves further investigation in the future.

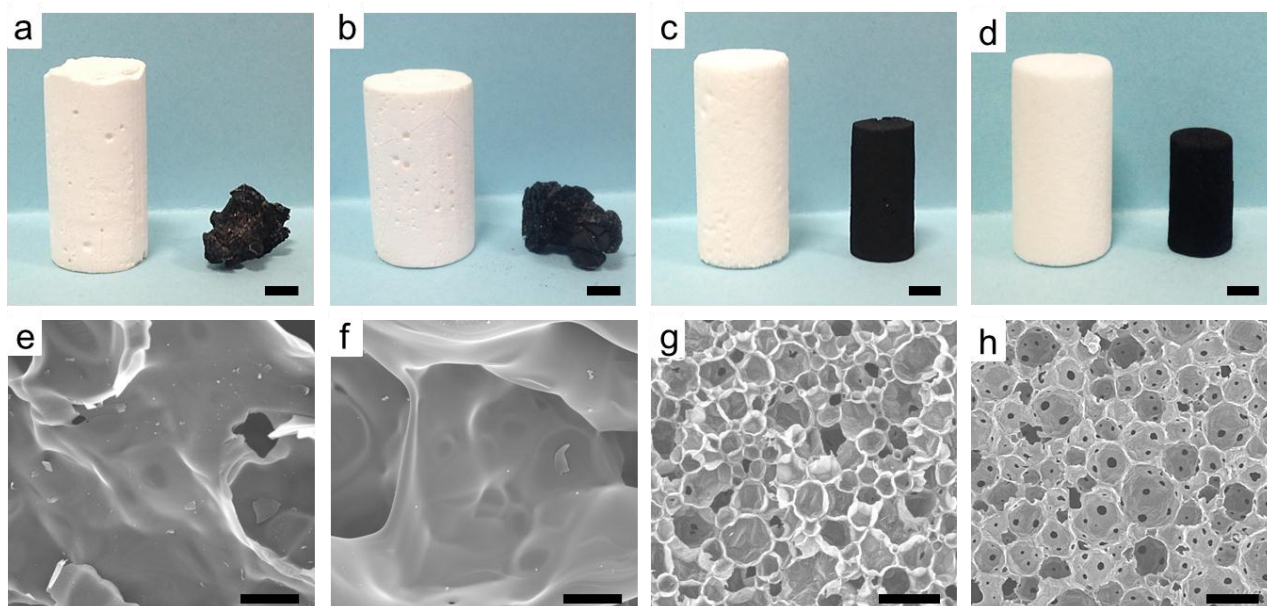


**Figure 3** (a) – (d) Photographs of polyHIPEs (white structures, left) and carboHIPEs (black structures, right) for materials sPH1, sPH2, pPH3 and psPH4, respectively. (e) – (h) SEM images of sPH1c, sPH2c, pPH3c and psPH4c, respectively. Scale bars represent 4 mm in (a) - (d) and 100  $\mu\text{m}$  in (e) - (h).

SEM images of the carbonized samples showed that both pPH3c and psPH4c carboHIPEs retained their emulsion-templated macroporosity throughout the entire structure (Figure 3g and h). On the other hand, sPH1c and sPH2c collapsed during carbonization, destroying the macroporous structure of the original polyHIPEs (Figure 3e,f), though some remnants of the original surfactant stabilised emulsion-templated structure remained intact (Figure S8), particularly on the top surface of the sPH1c and sPH2c. Quantification in SEM showed that the carbonization of pPH3 resulted in a reduction of the average pore diameter to around 54  $\mu\text{m}$  in pPH3c (Table 1), a drop of almost 15  $\mu\text{m}$ . The skeletal density of pPH3c and psPH4c increased after carbonization of the poly(DVB) to 1.54 and 1.83  $\text{g}/\text{cm}^3$ , respectively.

After pyrolysis, carboHIPEs pPH3c and psPH4c displayed increased BET surface areas (Table 1), as did the collapsed systems, sPH1c and sPH2c, which had BET surface areas of 658 m<sup>2</sup>/g and 572 m<sup>2</sup>/g, respectively. The isotherms of carboHIPEs sPH1c-pPH3c all showed a sharp uptake of N<sub>2</sub> at low relative pressures, indicative of newly formed micropores in all cases (Figure 4a-c). The pyrolysed sPH1 and sPH2 samples still showed some hysteresis on desorption, suggesting that although the HIPE templated macropores collapsed, some mesoporosity was retained. Both micro- and mesoporosity were confirmed by pore size distributions in sPH1c-pPH3c (Figure 4e), as measured using density functional theory methods. The degree of mesoporosity was slightly lower in pPH3c, reflected by the lack of hysteresis in the N<sub>2</sub> isotherm (Figure 4c), presumably due to the lack of mesoporosity in the pPH3 precursor. Despite exhaustive efforts, N<sub>2</sub> sorption was not possible for psPH4c samples due to very long equilibration times at low pressures ( $P/P_o < 1 \times 10^{-3}$ ). It was suspected that the pore-structure of psPH4c varied from that of the other samples, potentially creating pores too small to allow the use of N<sub>2</sub> as a suitable probe molecule. As an alternative, both argon (Figure 4d) and hydrogen (Figure S9) sorption experiments were performed; the argon isotherm again displayed a steep uptake of gas at low pressure, indicative of a microporous structure. The surface area of psPH4c was measured to be 115 m<sup>2</sup>/g, which is an increase from the polyHIPE precursor (50 m<sup>2</sup>/g) but much lower than that of the other carbon foams. Some hysteresis is observed in the isotherm, however it is not as pronounced as in sPH1c and sPH2c as a much smaller amount of molecular surfactant, also acting as a porogen, was used in this case. The hysteresis in the carbonized sample is in good agreement with the N<sub>2</sub> isotherm of psPH4, which showed a much less pronounced hysteresis than that of sPH1 and sPH2 (Figure 2). The H<sub>2</sub> isotherm showed similar behaviour, with a sharp uptake at low partial pressures and a H<sub>2</sub> uptake of 3.8 cm<sup>3</sup>/g at a partial pressure of 1 (Figure S9), confirming the porosity of psPH4c. Overall, the formation of micropores and subsequent dramatic increase in surface area is consistent with previous observations of carbonized polyDVB [34, 35].

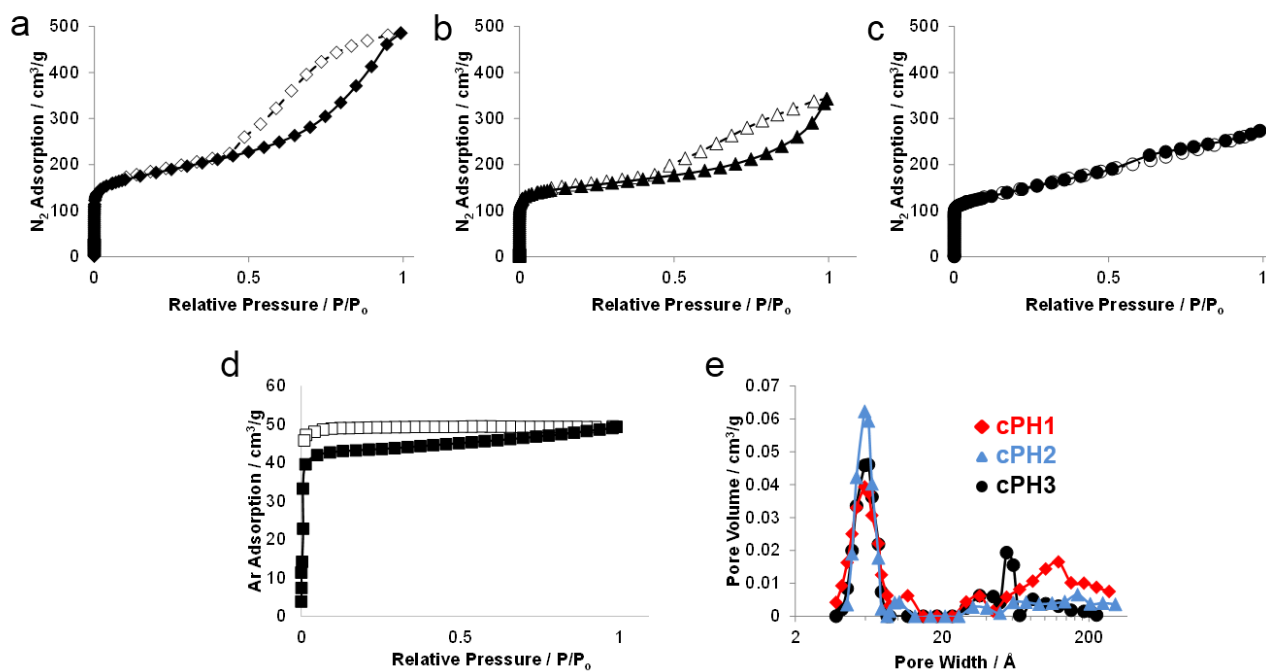


**Figure 4** N<sub>2</sub> isotherms of (a) sPH1c, (b) sPH2c and (c) pPH3c. (d) Argon isotherm of psPH4c. Filled shapes indicate adsorption and empty shapes indicate desorption in all isotherms. (e) Pore size distribution calculated using the density functional theory model for sPH1c (red diamonds), sPH2c (blue triangles) and pPH3c (black circles).

The ability of both pPH3 and psPH4 to retain their droplet-templated macroporosity upon carbonization seems to be linked to the presence of silica particles in the polyHIPE (seen in Figure 1g,h), which may act as a scaffold in the production of both closed- and open-cell carboHIPES, pPH3c and psPH4c, respectively. The lack of a scaffold of solid particles within sPH1 and sPH2 results in a less stable structure upon carbonization, leading to the collapse of the polyHIPES templated macropores. Initially, it was suspected that the collapse of sPH1 and sPH2 may also be attributed in part to the presence of the secondary pore structure within the poly(DVB)HIPE walls. However, when some mesoporosity was introduced into polyHIPES produced by polymerization of silica nanoparticle stabilized HIPEs, psPH4, the carboHIPES still retained their macroporosity well upon carbonization, suggesting that the presence of the particulate emulsifiers allows for the retention of the emulsion-templated macroporous structure rather than the lack of a secondary pore structure.

Raman spectroscopy can identify both polymeric and carbonaceous materials. The Raman spectra of polyHIPES both prior-to (Figure 5a) and post-carbonization (Figure 5b) show that carbonization led

to the loss of the fine structure of each polyHIPE's Raman spectrum and resulted in the appearance of the G and D modes ( $1582\text{ cm}^{-1}$  and  $1350\text{ cm}^{-1}$ , respectively) [46] that are typical of graphitic carbonaceous structures [47, 48] (Figure 5b). The fine structure of the polyHIPEs is in good agreement with those reported previously for poly(DVB) [49]. The ratio of peak intensities of D to G is around 1 in all cases, with broad peaks, indicating a disordered graphitic structure, as expected due to the low carbonization temperature [50]. The carbonization was confirmed using elemental analysis (Table S1) which showed increases in carbon to hydrogen ratio up to 100:1 from 10:1 upon carbonization in all samples.

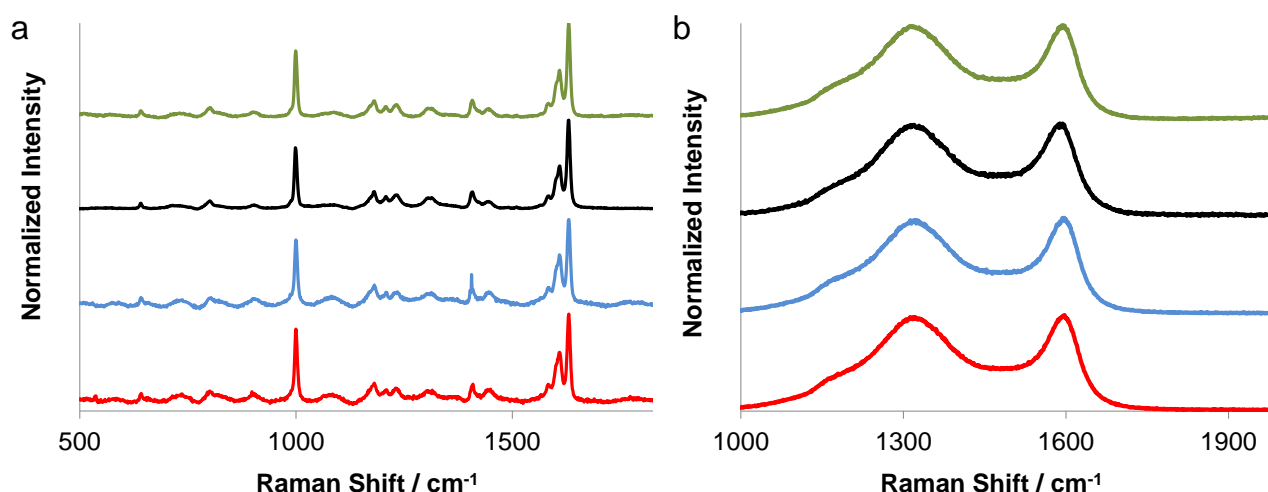


**Figure 5** Raman spectroscopy of sPH1 (red, bottom), sPH2 (blue, lower middle) and pH3 (black, upper middle) and psPH4 (green, top) a) prior to carbonization and b) after carbonization, showing the newly formed D ( $1350\text{ cm}^{-1}$ ) and G ( $1582\text{ cm}^{-1}$ ) peaks.

The well-defined shape and monolithic character of the carbonised pH3c and psPH4c samples allowed for accurate electrical conductivity measurements. Before carbonization, all polyHIPEs pH3 and psPH4 had conductivities lower than the measurement limit of the instrument ( $\sim 1 \times 10^{-7}\text{ S/m}$ ). However, a typical pH3c carboHIPE had conductivities of  $35\text{ S/m}$ , displaying a huge increase in electrical conductivity after carbonization. This value increases again slightly in the permeable carboHIPE, psPH4c, to  $81\text{ S/m}$ , amongst the highest reported for carbon foams derived from polyHIPE precursors. The conductivity of pH3c is comparable to that of resorcinol

formaldehyde carboHPIEs of similar porosity (up to 34 S/m for 87 % porosity) [22]. It is almost double the conductivity measured [24] for a furifural and phloroglucinol based carboHIPE with a porosity of 98 % when carbonized at 750 °C, however the conductivity of this system increases to 300 S/m when carbonized at temperatures of 950 °C. Although a number of different carboHPIEs are known, most studies do not report electrical conductivity, making it difficult to compare these results with similar materials. In any case, the conductivity sensitivity depends on porosity and carbonisation/graphitization temperature.

#### **4. Conclusions**

A simple route for the production of conducting, hierarchically porous carbon foams has been demonstrated; poly(DVB)HPIEs, synthesized by polymerization of particle-stabilized w/o HPIEs, are stable precursors for the production of carboHPIEs by pyrolysis. The incorporation of silica particles into the pore walls of the polyHIPE precursors provided a robust scaffold for the production of both closed- and open-cell carboHPIEs. In contrast, the emulsion-templated macroporous structure of the molecular surfactant stabilised polyHPIEs is largely destroyed upon carbonization. This collapse may be due to the absence of the inorganic silica particles in the pore walls of the polyHPIEs. When a mixed surfactant system (i.e. pSPH4) is used to create a carbon foam, the emulsion-templated macroporosity is still retained upon carbonization even with the presence of a secondary pore structure in the material, suggesting that in the mixed emulsifier system the presence of the particulate emulsifiers is dominant. The resulting carboHIPE monoliths contain emulsion-templated macroporosity, as well as mesopores and micropores from the intrinsic carbonisation of DVB. These carboHPIEs display conductivities up to 81 S/m and surface areas up to 505 m<sup>2</sup>/g, without the need for post-polymerization treatments such as cross-linking, or the removal of inorganic-templates using harsh chemicals such as hydrofluoric acid, post-carbonization. This simple pourable w/o-HIPE provides a cost effective route to monolithic carboHPIEs with the potential to create a wide variety



of moulded structures. In principle, the pore size of the carboHIPEs could be adjusted by varying the size and wettability of the particulate emulsifier. In fact, a wide variety of (nano)particulates could be considered, as long as they have sufficient thermal stability, offering the opportunity to embed different functional materials into the surface of the resulting carboHIPE. These mouldable carboHIPEs have potential applications as catalyst supports, in water purification and as electrodes in electrochemical energy conversion devices (supercapacitors, fuel cells, etc), due to their relatively low cost, high surface areas and excellent electrical conductivity.

## **Acknowledgements**

We wish to thank Patricia Carry (Imperial College London) for assistance with both the poly(DVB)HIPE BET surface area measurements and the skeletal density measurements and Rob Clowes (The University of Liverpool) for assistance with all isotherms ran on psPH4c samples. We would also like to thank Hin Chun Yau (Imperial College London) and Johannes Theiner (University of Vienna) for assistance with elemental analysis measurements and François De Luca for assistance with the high magnification SEM images. We gratefully acknowledge funding from the UK Engineering and Physical Sciences Research Council (EPSRC) through the projects “graphene 3D networks” (EP/K01658X/1) and “platform grant” (EP/J014974/1).

## **References**

- [1] Yu JS, Kang S, Yoon SB, Chai G. Fabrication of ordered uniform porous carbon networks and their application to a catalyst supporter. *J Am Chem Soc* 2002;124:9382-3.
- [2] Rodriguez-Reinoso F. The role of carbon materials in heterogeneous catalysis. *Carbon* 1998;36:159-75.
- [3] Saufi SM, Ismail AF. Fabrication of carbon membranes for gas separation - a review. *Carbon* 2004;42:241-59.
- [4] Kim HW, Yoon HW, Yoon SM, Yoo BM, Ahn BK, Cho YH, et al. Selective Gas Transport Through Few-Layered Graphene and Graphene Oxide Membranes. *Science* 2013;342:91-5.
- [5] Chung DDL. Electromagnetic interference shielding effectiveness of carbon materials. *Carbon* 2001;39:279-85.
- [6] Al-Saleh MH, Sundararaj U. Electromagnetic interference shielding mechanisms of CNT/polymer composites. *Carbon* 2009;47:1738-46.
- [7] Shannon MA, Bohn PW, Elimelech M, Georgiadis JG, Marinas BJ, Mayes AM. Science and technology for water purification in the coming decades. *Nature* 2008;452:301-10.

- [8] Zhang LL, Zhao XS. Carbon-based materials as supercapacitor electrodes. *Chem Soc Rev* 2009;38:2520-31.
- [9] Frackowiak E, Beguin F. Carbon materials for the electrochemical storage of energy in capacitors. *Carbon* 2001;39:937-50.
- [10] Hu YS, Adelhelm P, Smarsly BM, Hore S, Antonietti M, Maier J. Synthesis of hierarchically porous carbon monoliths with highly ordered microstructure and their application in rechargeable lithium batteries with high-rate capability. *Advanced Functional Materials* 2007;17:1873-8.
- [11] Roberts AD, Li X, Zhang HF. Porous carbon spheres and monoliths: morphology control, pore size tuning and their applications as Li-ion battery anode materials. *Chem Soc Rev* 2014;43:4341-56.
- [12] Lee J, Kim J, Hyeon T. Recent progress in the synthesis of porous carbon materials. *Advanced Materials* 2006;18:2073-94.
- [13] Stein A, Wang ZY, Fierke MA. Functionalization of Porous Carbon Materials with Designed Pore Architecture. *Advanced Materials* 2009;21:265-93.
- [14] Barby D, Haq Z. Low density porous cross-linked polymeric materials and their preparation In: Office EP, editor.1982.
- [15] Cameron NR, Sherrington DC. High internal phase emulsions (HIPEs) - Structure, properties and use in polymer preparation. *Biopolymers Liquid Crystalline Polymers Phase Emulsion* 1996;126:163-214.
- [16] Cohen N, Silverstein MS. Synthesis of emulsion-templated porous polyacrylonitrile and its pyrolysis to porous carbon monoliths. *Polymer* 2011;52:282-7.
- [17] Szczurek A, Fierro V, Pizzi A, Celzard A. Emulsion-templated porous carbon monoliths derived from tannins. *Carbon* 2014;74:352-62.
- [18] Ungureanu S, Sigaud G, Vignoles GL, Lorrette C, Birot M, Deleuze H, et al. First Biosourced Monolithic Macroporous SiC/C Composite Foams (Bio-SiC/C(HIPE)) Bearing Unprecedented Heat Transport Properties. *Advanced Engineering Materials* 2013;15:893-902.
- [19] Ungureanu S, Birot M, Deleuze H, Schmitt V, Mano N, Backov R. Triple Hierarchical Micro-Meso-Macroporous Carbonaceous Foams Bearing Highly Monodisperse Macroporosity. *Carbon* 2015.
- [20] Brun N, Prabakaran SRS, Morcrette M, Sanchez C, Pecastaings G, Derre A, et al. Hard Macrocellular Silica Si(HIPE) Foams Templating Micro/Macroporous Carbonaceous Monoliths: Applications as Lithium Ion Battery Negative Electrodes and Electrochemical Capacitors. *Advanced Functional Materials* 2009;19:3136-45.
- [21] Liu M, Gan L, Zhao F, Xu H, Fan X, Tian C, et al. Carbon foams prepared by an oil-in-water emulsion method. *Carbon* 2007;45:2710-2.
- [22] Gross AF, Nowak AP. Hierarchical Carbon Foams with Independently Tunable Mesopore and Macropore Size Distributions. *Langmuir* 2010;26:11378-83.
- [23] Thongprachan N, Yamamoto T, Chaichanawong J, Ohmori T, Endo A. Preparation of macroporous carbon foam using emulsion templating method. *Adsorption-Journal of the International Adsorption Society* 2011;17:205-10.
- [24] Brun N, Edembe L, Gounel S, Mano N, Titirici MM. Emulsion-Templated Macroporous Carbons Synthesized By Hydrothermal Carbonization and their Application for the Enzymatic Oxidation of Glucose. *Chemsuschem* 2013;6:701-10.
- [25] Vilchez S, Perez-Carrillo LA, Miras J, Solans C, Esquena J. Oil-in-Alcohol Highly Concentrated Emulsions as Templates for the Preparation of Macroporous Materials. *Langmuir* 2012;28:7614-21.
- [26] Alam MM, Miras J, Perez-Carrillo LA, Vilchez S, Solans C, Imae T, et al. Facile synthesis of dual micro/macroporous carbonaceous foams by templating in highly concentrated water-in-oil emulsions. *Microporous and Mesoporous Materials* 2013;182:102-8.
- [27] Zhang HF, Cooper AI. Synthesis and applications of emulsion-templated porous materials. *Soft Matter* 2005;1:107-13.
- [28] Cameron NR. High internal phase emulsion templating as a route to well-defined porous polymers. *Polymer* 2005;46:1439-49.
- [29] Wang D, Smith NL, Budd PM. Polymerization and carbonization of high internal phase emulsions. *Polymer International* 2005;54:297-303.
- [30] Israel S, Gurevitch I, Silverstein MS. Carbons with a hierarchical porous structure through the pyrolysis of hypercrosslinked emulsion-templated polymers. *Polymer* 2015;72:453-63.
- [31] Hainey P, Huxham IM, Rowatt B, Sherrington DC, Tetley L. SYNTHESIS AND ULTRASTRUCTURAL STUDIES OF STYRENE DIVINYLBENZENE POLYHIPE POLYMERS. *Macromolecules* 1991;24:117-21.

- [32] Pakeyangkoon P, Magaraphan R, Malakul P, Nithitanakul M. Effect of Soxhlet extraction and surfactant system on morphology and properties of Poly(DVB)PolyHIPE. *Macromolecular Symposia* 2008;264:149-56.
- [33] Williams JM, Gray AJ, Wilkerson MH. EMULSION STABILITY AND RIGID FOAMS FROM STYRENE OR DIVINYLBENZENE WATER-IN-OIL EMULSIONS. *Langmuir* 1990;6:437-44.
- [34] Jang J, Lim B. Selective fabrication of carbon nanocapsules and mesocellular foams by surface-modified colloidal silica templating. *Advanced Materials* 2002;14:1390-3.
- [35] Yoon SB, Kim JY, Yu JS. Synthesis of highly ordered nanoporous carbon molecular sieves from silylated MCM-48 using divinylbenzene as precursor. *Chem Commun* 2001:559-60.
- [36] Cameron NR, Sherrington DC, Albiston L, Gregory DP. Study of the formation of the open cellular morphology of poly(styrene/divinylbenzene) polyHIPE materials by cryo-SEM. *Colloid Polym Sci* 1996;274:592-5.
- [37] Menner A, Verdejo R, Shaffer M, Bismarck A. Particle-stabilized surfactant-free medium internal phase emulsions as templates for porous nanocomposite materials: Poly-pickering-foams. *Langmuir* 2007;23:2398-403.
- [38] Menner A, Ikem V, Salgueiro M, Shaffer MSP, Bismarck A. High internal phase emulsion templates solely stabilised by functionalised titania nanoparticles. *Chem Commun* 2007:4274-6.
- [39] Menner A, Bismarck A. New evidence for the mechanism of the pore formation in polymerising High Internal Phase Emulsions or why polyHIPEs have an interconnected pore network structure. *Macromol Symp* 2006;242:19-24.
- [40] Ikem VO, Menner A, Bismarck A. High Internal Phase Emulsions Stabilized Solely by Functionalized Silica Particles. *Angewandte Chemie-International Edition* 2008;47:8277-9.
- [41] Ikem VO, Menner A, Horozov TS, Bismarck A. Highly Permeable Macroporous Polymers Synthesized from Pickering Medium and High Internal Phase Emulsion Templates. *Advanced Materials* 2010;22:3588-+.
- [42] Schneider CA, Rasband WS, Eliceiri KW. NIH Image to ImageJ: 25 years of image analysis. *Nature Methods* 2012;9:671-5.
- [43] Binks BP. Particles as surfactants - similarities and differences. *Current Opinion in Colloid & Interface Science* 2002;7:21-41.
- [44] Wong LLC, Ikem VO, Menner A, Bismarck A. Macroporous Polymers with Hierarchical Pore Structure from Emulsion Templates Stabilised by Both Particles and Surfactants. *Macromolecular Rapid Communications* 2011;32:1563-8.
- [45] Sing KSW, Everett DH, Haul RAW, Moscou L, Pierotti RA, Rouquerol J, et al. REPORTING PHYSISORPTION DATA FOR GAS SOLID SYSTEMS WITH SPECIAL REFERENCE TO THE DETERMINATION OF SURFACE-AREA AND POROSITY (RECOMMENDATIONS 1984). *Pure Appl Chem* 1985;57:603-19.
- [46] Dresselhaus MS, Dresselhaus G, Saito R, Jorio A. Raman spectroscopy of carbon nanotubes. *Phys Rep-Rev Sec Phys Lett* 2005;409:47-99.
- [47] Ferrari AC. Raman spectroscopy of graphene and graphite: Disorder, electron-phonon coupling, doping and nonadiabatic effects. *Solid State Commun* 2007;143:47-57.
- [48] Ferrari AC, Robertson J. Interpretation of Raman spectra of disordered and amorphous carbon. *Phys Rev B* 2000;61:14095-107.
- [49] Stokr J, Schneider B, Frydrychova A, Coupek J. COMPOSITION ANALYSIS OF CROSSLINKED STYRENE-ETHYLENE DIMETHACRYLATE AND STYRENE-DIVINYLBENZENE COPOLYMERS BY RAMAN-SPECTROSCOPY. *Journal of Applied Polymer Science* 1979;23:3553-61.
- [50] Jiangling L, Shi S, Lei Z, Abbot AM, Ye H. Dielectric transition of polyacrylonitrile derived carbon nanofibers. *Mater Res Express* 2014;1:035604 (9 pp.)- (9 pp.).